

Out-of-Plane Shaking Table Test of a Full Scale Stone Masonry Façade



A.A. Costa & A. Arêde

Faculty of Engineering, University of Porto, Portugal

A.C. Costa

Laboratório Nacional de Engenharia Civil, Portugal

A. Penna

University of Pavia, Italy

A. Costa

University of Aveiro, Portugal

SUMMARY:

The out-of-plane behaviour of stone masonry façades is a major cause of several collapses during seismic events. For this reason, the work presented herein refers to a shaking table test performed on a full scale one-storey stone masonry façade, representative of an existing building from Faial island (Azores, Portugal). All the test protocol and procedure is described as well as a presentation of the overall behaviour and obtained results. Moreover, since the selection of a ground motion able to trigger the out-of-plane mode was a crucial point for the seismic test, the method used to select the input motion is also addressed in the present paper.

Keywords: shaking table, stone masonry, out-of-plane, full scale.

1. INTRODUCTION

Observing several post-earthquake damages among different areas and time periods, out-of-plane collapses of masonry walls are commonly found, including recent events (e.g. L'Aquila 2009 earthquake). Despite being a well-known problem, experimental tests specifically focused on the out-of-plane behaviour of masonry structures resorting to shaking table tests are not common.

Although the out-of-plane behaviour of masonry walls are observed in more general shaking table tests (e.g. (Tomazevic *et al.* 1996; Magenes *et al.* 2010)), only the recent works by D'Ayala *et al.* (2011) and Al Shawa *et al.* (2011) addressed specifically the out-of-plane behaviour, the latter on a full scale tuff masonry specimen.

Regarding out-of-plane shaking table tests on *sacco* stone masonry walls as commonly observed in Portugal as well as in the Mediterranean area, no out-of-plane shaking table tests were found, increasing the research interest in this area.

For the reasons mentioned above, and bearing in mind the vulnerability of stone masonry constructions, the dynamic out-of-plane behaviour of *sacco* stone masonry walls should be studied and supported by experimental evidence based on the shaking table tests.

2. SPECIMEN AND SHAKING TABLE TEST SETUP

The assessment of the out-of-plane dynamic behaviour of a *sacco* stone masonry façade was made resorting to the LNEC (Laboratório Nacional de Engenharia Civil, Lisbon, Portugal) tri-axial shaking table. Despite the possibility to introduce a 3D motion on the table, only the transversal axis, perpendicular to the main façade, was used in order to study specifically the out-of-plane problem. A realistic full scale specimen was selected, conveying a partial reproduction of an existing construction from Faial island, Azores, and similar to damaged and collapsed structures found after the 1998 Azores earthquake.

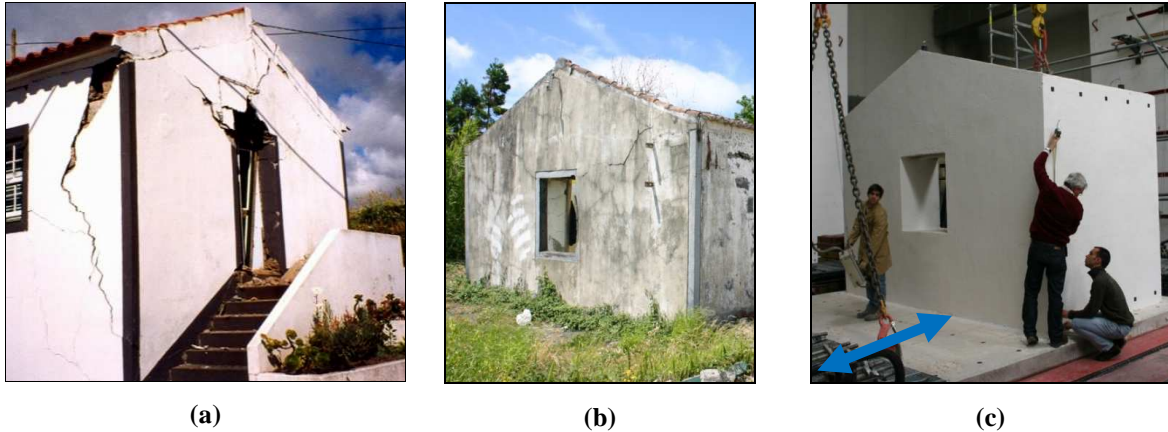


Figure 2.1. Specimen reproduced on the shaking table tests: a) damage construction after 1998 Azores earthquake; b) original specimen in Azores; c) specimen at LNEC shaking table and direction of motion.

The construction of the specimen was made by local masons familiar to work on this type of structures, respecting traditional construction techniques. Attempting to reproduce also the wall's typology from Azores, walls were built as *sacco* stone masonry (double leaf masonry with poor infill material), made of granite blocks and lime mortar, leading to a total thickness of 65cm. The building roof was not included in the specimen because, in the traditional construction from Azores island, the roof is supported at the front and rear walls and therefore no vertical load is introduced in the wall (lateral one) tested in this shaking table test.

Regarding the geometry of the tested specimen, a main façade with two returning walls was adopted, as depicted in Figure 2.1, with poor interlocking between the main façade and perpendicular walls aiming at activating the façade overturning with minimized the flexural behaviour.

The main specimen dimensions are presented in Figure 2.2 a) while the monitoring points are shown in Figure b). The returning walls were 2.15 meter long.

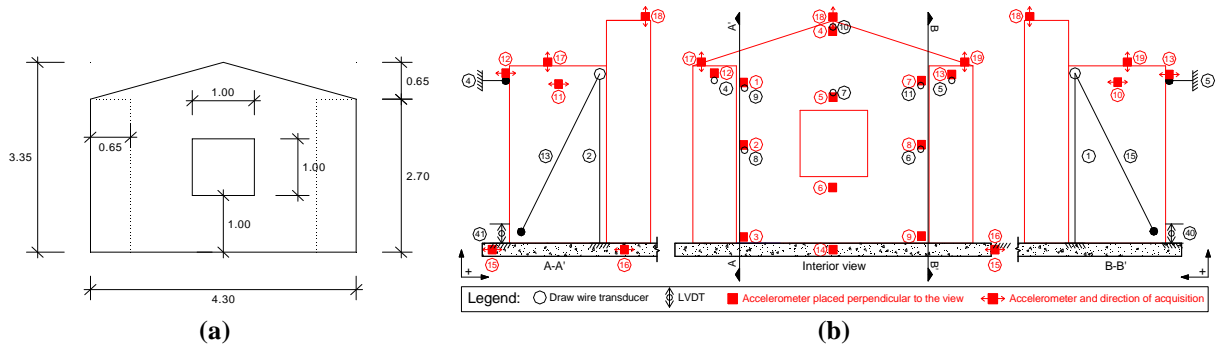


Figure 2.2. Characteristics of the tested specimen: a) dimensions; b) monitoring points and devices

Concerning the instrumentation used to characterize the out-of-plane behaviour, 13 displacement transducers (more precisely draw wire position transducers), 2 LVDTs and 19 accelerometers were adopted for the tested specimen; in addition to 3 full HD video cameras (25 frames per second) were used as well as 3 medium speed full HD (50 frames per second) and 1 high speed (120 frames per second) VGA camera.

From the observation of the recorded videos, it was possible to make a detailed interpretation of the behaviour exhibited by the specimen during the shaking table tests, by correlating visual observations with the acquired experimental data.

3. SELECTION OF THE GROUND MOTION

The selection of the ground motion revealed to be a crucial point of the work presented herein, because the accelerogram to be used on the shaking table should trigger the out-of-plane mechanism without inducing severe damage to the specimen. Moreover, it should be also referred that the main objective of the shaking table was to induce the complete collapse of the main façade, characterizing the overturning activation as well as the out-of-plane collapse.

The overturning of masonry walls is correlated to the input kinetic energy, which can be associated to near-fault characteristics of the ground motion, especially the velocity pulses (forward, backward or forward-backward) usually observed in this type of events. This statement was verified through numerical simulations by Decanini *et al.* (2006) where velocity measures, as Peak Ground Velocity (PGV) and Housner intensity have good correlation with the overturning of rigid bodies under earthquake actions. The simulation of the out-of-plane behaviour of masonry walls may be achieved by rigid elements rocking around its base and, therefore, its potential overturning is given also by the slenderness of the walls. While PGV (Decanini *et al.* 2006) or maximum spectral displacement (Liberatore *et al.* 2009) give an idea of potential overturning and possible damage on rocking bodies, PGA is the main parameter involved in squat walls' response where higher accelerations are required to activate rocking.

However, there is no simple correlation between a single parameter related to the seismic motion and the overturning potential of the masonry wall. Hence, the selection of the accelerogram to be used on the shaking table should be made resorting to an analysis which may simulate the overturning potential of the seismic motion and the tested specimen.

In order to select a ground motion with overturning potential of the masonry façade, a step-by-step procedure was defined and followed, as represented in Figure 3.1, starting from the selection of a set of potential accelerograms.

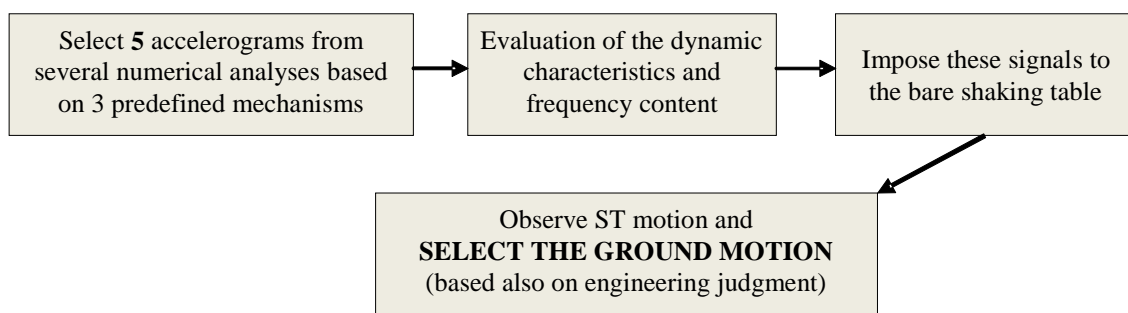


Figure 3.1. Step-by-step procedure to select the ground motion

Thus, an initial selection was made of the potential accelerograms to be used in the shaking table, resulting in a set of 74 accelerograms: 70 from Reluis project (more information available in Decanini *et al.* (2006)); 1 record of the 9 July 1998 Azores earthquake (HOR, NS and WE components) and 1 record of the 6 April 2009 L'Aquila (FA090-AQG, NS and WE components).

With the initial set of accelerograms, three potential collapse mechanisms were selected based on the specimen's geometry and presented in Figure 3.2, in accordance with existing proposals based on geometrical properties (Lagomarsino 1998).

Numerical models were then developed with the considered mechanisms in order to analyse the potential overturning of the ground motion for each potential mechanism.

The numerical models presented in Figure 3.2 were divided in two different masonry portions: *i*) one rigid element representative of the potential overturning mechanism (yellow parts); *ii*) the other masonry portions, which involved the remaining part of the specimen, were fixed to the shaking table and considered infinitely rigid.

In order to perform nonlinear dynamic analysis, the MSC Adams™ (Multibody Dynamics Simulation, Automatic Dynamic Analysis of Mechanical Systems) software (MSC 2012) was used, adopting rigid

bodies to simulate the masonry portions, while concentrated nonlinearity at the contact regions in the form of friction and of a restitution coefficient which traduces the energy dissipation on impacts between different elements.

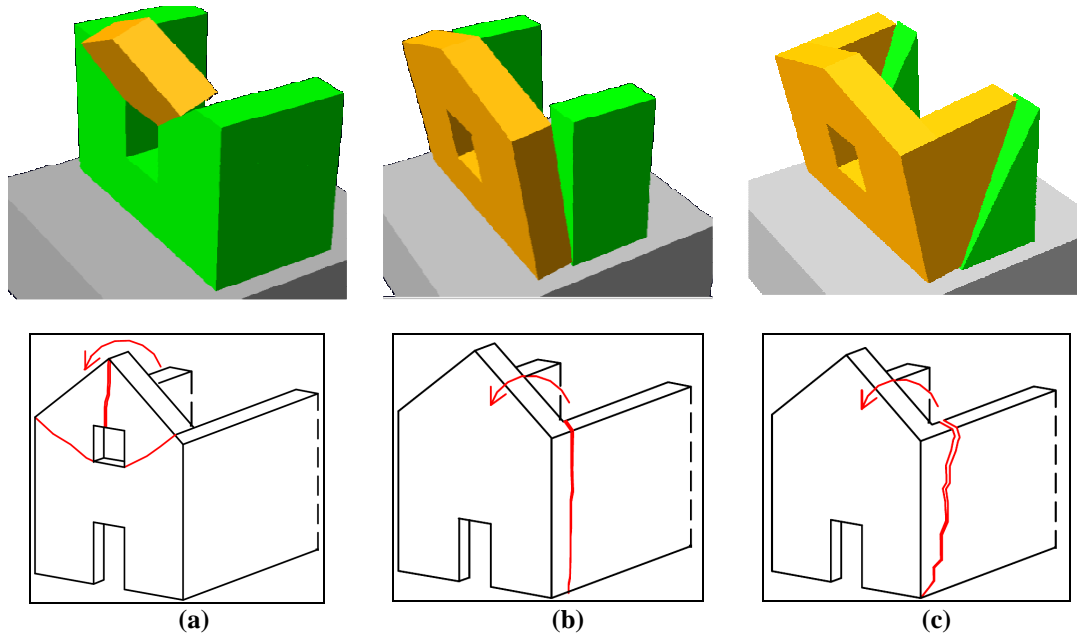


Figure 3.2. Potential overturning mechanisms considered in the numerical analyses and correspondence with existing proposal (Lagomarsino 1998): a) gable (MEC0); b) façade (MEC1); c) façade with returning walls (MEC2).

Finally, the parameters required to perform dynamic analyses were only the rigid bodies' unit weight, the friction and restitution coefficients (divided in horizontal and vertical impacts), which were selected based on literature values as presented in Table 3.1.

Table 3.1. Parameters used in the preliminary numerical analysis

Specific weight (ρ) (kN/m^3)	Static and dynamic friction coefficient (μ)	Coefficient of restitution (r)
19.0 (Costa 2002; NTC 2008)	0.7 (Vasconcelos <i>et al.</i> 2009)	0.1

After the numerical models development, all the 74 ground motions were used as input motions at the base of models, being all the accelerograms scaled to 0.6g, a value sufficiently high to trigger all the mechanisms and to observe the potential collapse induced by some of the accelerograms. From the set of 74 ground motions, 4 were identified as potential input motions from the displacement obtained in the numerical analysis, as well as the L'Aquila's NS record (which was selected because it is a recent record, where several out-of-plane collapses were observed in the Abruzzo region, Italy). The main displacement ratios (δ/Δ_u , where δ is the displacement obtained in the numerical model and Δ_u is the instability displacement) are presented in Table 3.2.

Table 3.2. Displacements obtained in the numerical analysis for the selected records

Earthquake	Record	M_w	D_f [km]	PGA (g)	PGV (cm/s)	Displacement ratio (δ/Δ_u)		
						MEC0	MEC1	MEC2
Northridge	NWH360	6.7	4.0	0.59	96.9	0.07	0.42	0.11
Loma Prieta	HOLL0	6.9	33.0	0.37	63.0	0.10	Collapse	0.19
Loma Prieta	A02043	6.9	47.4	0.27	53.6	0.09	0.74	0.11
Loma Prieta	HCH180	6.9	27.8	0.21	45.0	0.02	0.87	0.10
L'Aquila	AQG (NS)	5.8	4.3	0.49	35.7	0.00	0.02	0.00

As presented in Figure 3.1, the selection of the ground motion was made on three different steps: *i*) selection of 5 potential accelerograms, based on the numerical results; *ii*) observation of response spectra of the 5 selected ground motions, evaluating the frequency content; *iii*) introduction of the ground motions on the bare shaking table and observation of the shaking table movements, selecting the most adequate accelerogram to be used.

At the end of the selection procedure, it was adopted the 1994 Northridge earthquake recorded at Newhall Fire station (NWH360), filtered at long period vibration ($f_{cut} = 0.2$ Hz) in order to fully explore the limits of the shaking table without affecting the final results. Moreover, this accelerogram was possible to be scaled down for different intensity levels, while the other records should be scaled up in order to have higher PGA values.

The final input ground motion used on the shaking table tests is presented in Figure 3.3.

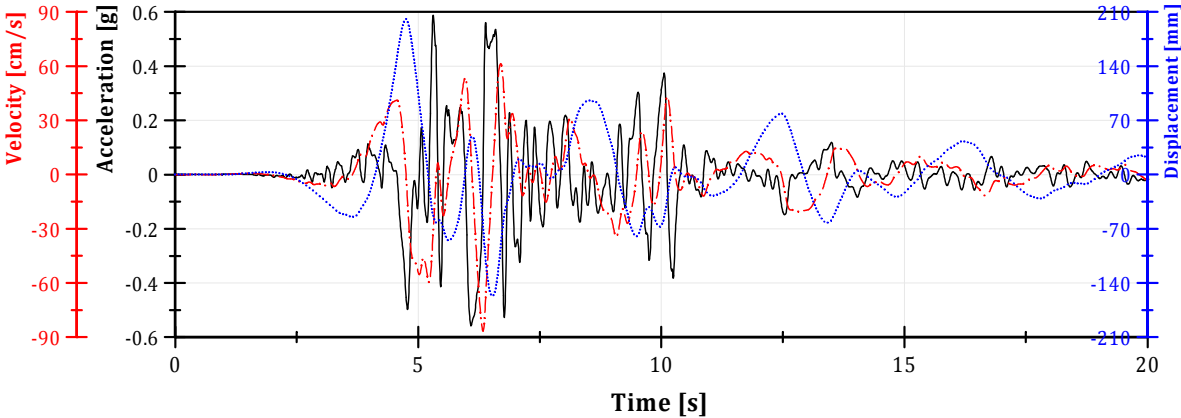


Figure 3.3. Input ground motion for the shaking table tests: 17 January 1994 Northridge earthquake recorded at Newhall Fire station (NWH360) filtered at low frequencies

Five different levels of the ground motion were introduced at the shaking table, as percentages of the full scale signal: 1) 10%; 2) 20%; 3) 40%; 4) 60%; 5) 80%. The response spectra of the input ground motion (NWH360 original signal) and measured data are presented in Figure 3.4 for each test stage, where it is possible to observe the good response of the shaking table when compared to the original signal.

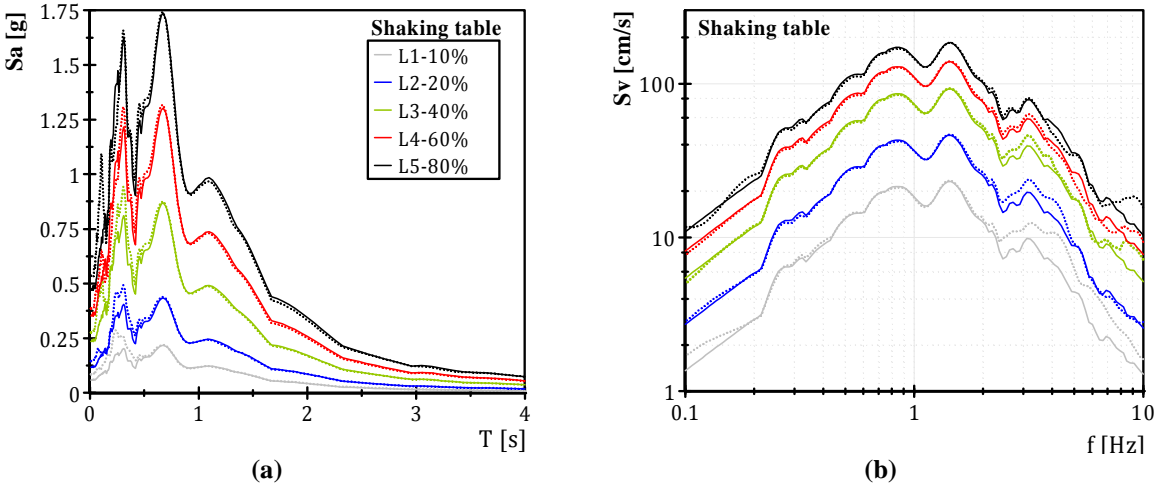


Figure 3.4. Response spectra for different levels of ground motion: comparison between input motion and acquired data (solid lines, input; dot lines, measured); a) acceleration spectra; b) pseudo-velocity.

4. EXPERIMENTAL RESULTS AND DATA INTERPRETATION

During the seismic testing campaign, the behaviour of the specimen may be divided in two different stages: before stage L3 (scale factor 40%); after stage L3. As presented in Table 4.1, the specimen did not exhibit damage until the stage L3. After this stage level, the formation of the overturning mechanism occurred for stage L4 (60%), where the detachment of the façade occurred at the window level with a triangular shape.

At the final stage of the shaking table campaign, the collapse of the masonry façade occurred with well defined overturning of the masonry façade above the window level, as shown in Figure 4.1. After the detachment between the façade and returning walls (Figure 4.1 a)), the collapse was mainly caused by the instability of the outer leaf, induced by the presence of window frame. If Figure 4.1 b) is observed more carefully, the rotation of the window jamb stones is visible and, due to their vertical orientation, the instability of these elements became easily achieved. This local instability led to the collapse of the complete wall façade also due to global instability, with the final collapse form of Figure 4.1 c).

Table 4.1. Description of the damage evolution

Stage	Scale factor	Behaviour of the façade	Damage and observed behaviour
L1	10%	Monolithic	No visible damage
L2	20%	Monolithic	No visible damage
L3	40%	Flexural response	Small vertical cracks at the façade and diagonal cracks in returning walls
L4	60%	Rigid body motion (one-sided rocking)	Façade detachment at the window level (1.0 meter) and cracks at the gable
L5	80%	Rigid body motion with overturning	Façade collapse caused by instability of the outer leaf at window level

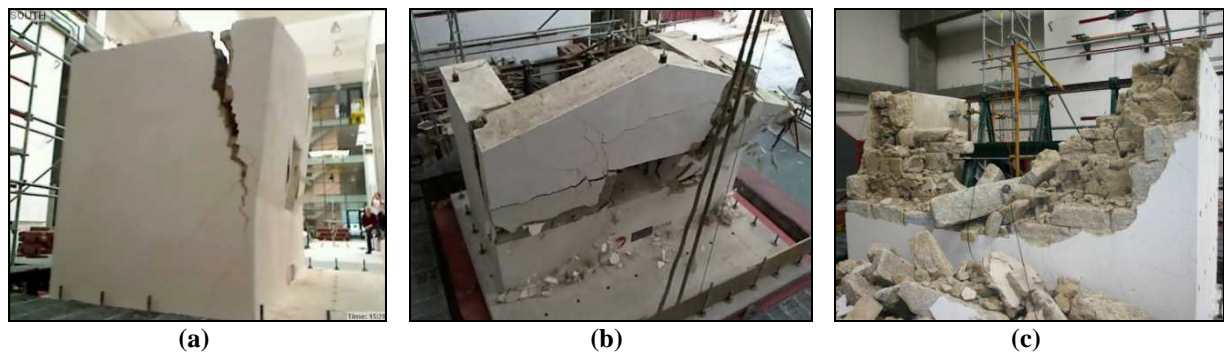


Figure 4.1. Overturning and collapse mechanism: a) formation of the mechanism; b) collapse development; c) final collapse figure at stage L5 (80%).

The façade top displacement time history (measured by the wire transducer 10, in Figure 2.2 b)) is presented in Figure 4.2, where the out-of-plane behaviour of the façade is visible. The 40% signal did not induce any considerable displacement in the wall ($\delta_{\max} = 5.1$ mm). However, the 60% scaled signal triggered the out-of-plane mechanism (for the time step 6.5 s), thus increasing the façade flexibility as evidenced in Figure 4.2. After that time step, the displacement increased significantly and it became possible to observe the façade rocking behaviour. The 80% signal led to the out-of-plane collapse of the wall as mentioned previously.

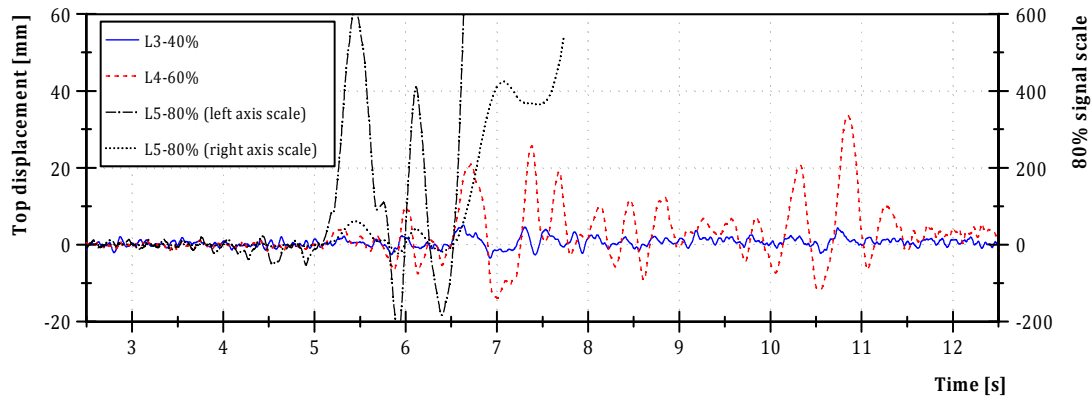


Figure 4.2. Top displacement time histories for 40%, 60% and 80%.

The façade collapse occurred when the out-of-plane top displacement achieved 400 mm (or approximately 60% Δ_u , where Δ_u is the instability displacement). However, because the collapse was achieved due to the outer leaf instability, a limit displacement similar to the outer leaf (≈ 250 mm) may be more representative of the ultimate displacement for this type of walls. Therefore, displacement-based assessment procedures concerning the out-of-plane behaviour of multiple leaves masonry walls should consider the instability of the wall governed by the thickness of the outer leaf.

Figure 4.3 presents the top acceleration vs. top displacement where the hysteretic behaviour of the masonry façade can be observed. In the same line as previously mentioned, the figure shows that the 40% signal started to induce some nonlinearity, which significantly increased in the L4 test (60%). As expected, the maximum acceleration is higher in the positive sense due to the presence of the returning walls, reflected also in the achieved displacement (smaller in the negative sense when compared to positive ones). The curves shape shows a peak negative acceleration value of -0.62 g (achieved at L4 stage) which can be the threshold acceleration to form the overturning mechanism. The stiffness and strength degradation is also observable but it is influenced, in the positive displacement sense, by façade rocking behaviour rather than flexural response which may lead to misinterpreted stiffness evaluation.

At the last test level, the behaviour is characterized by strong nonlinearity with stiffness and strength degradation when compared to previous test stages. It can be observed that a constant acceleration level around -0.22 g induced the collapse of the specimen, which is consistent with the threshold acceleration value required for the out-of-plane mechanism (0.23 g) that can be computed based on the geometry of the activated masonry block (Costa 2012).

As a general comment, the maximum strength was achieved for 0.3% drift, while the estimated ultimate displacement of 1.2% drift was reached.

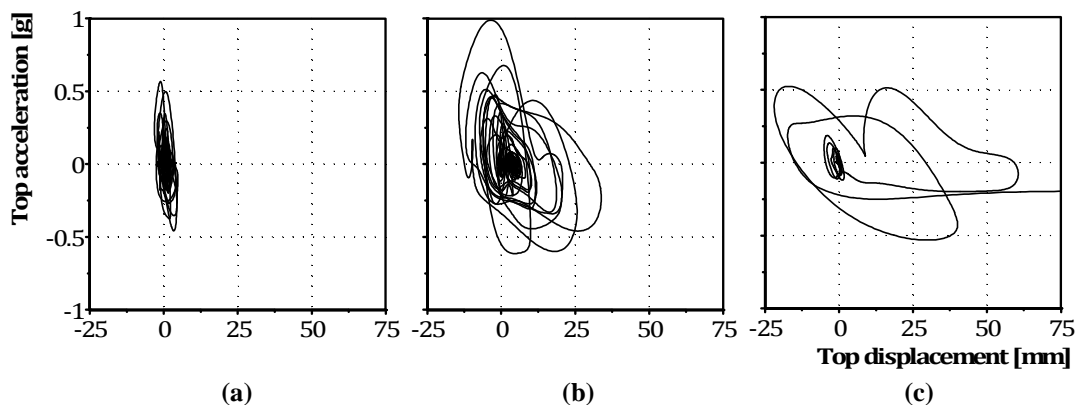


Figure 4.3: Top absolute acceleration vs. top displacement: a) L3-40%; b) L4-60%; c) L5-80%.

The velocity time histories, shown in Figure 4.4 for the vertical profile of accelerometers placed at the centre line of the main façade, are consistent with the rocking behaviour of the masonry façade, highlighting this type of behaviour with experimental data.

Indeed, it is possible to observe the façade rocking behaviour in the results of stage L4, showing in-phase responses at the top and window levels, with maximum velocity of 50cm/s; by contrast, out-of-phase response of velocities is observed in stage L5, reaching maximum velocity of 65cm/s before attaining the collapse, which suggests that the motion modified the rocking point axis position in the façade plane.

Thus, it may be possible to infer that a minimum velocity pulse of 60-65 cm/s was required to induce sufficient kinetic energy for the global overturning of the façade.

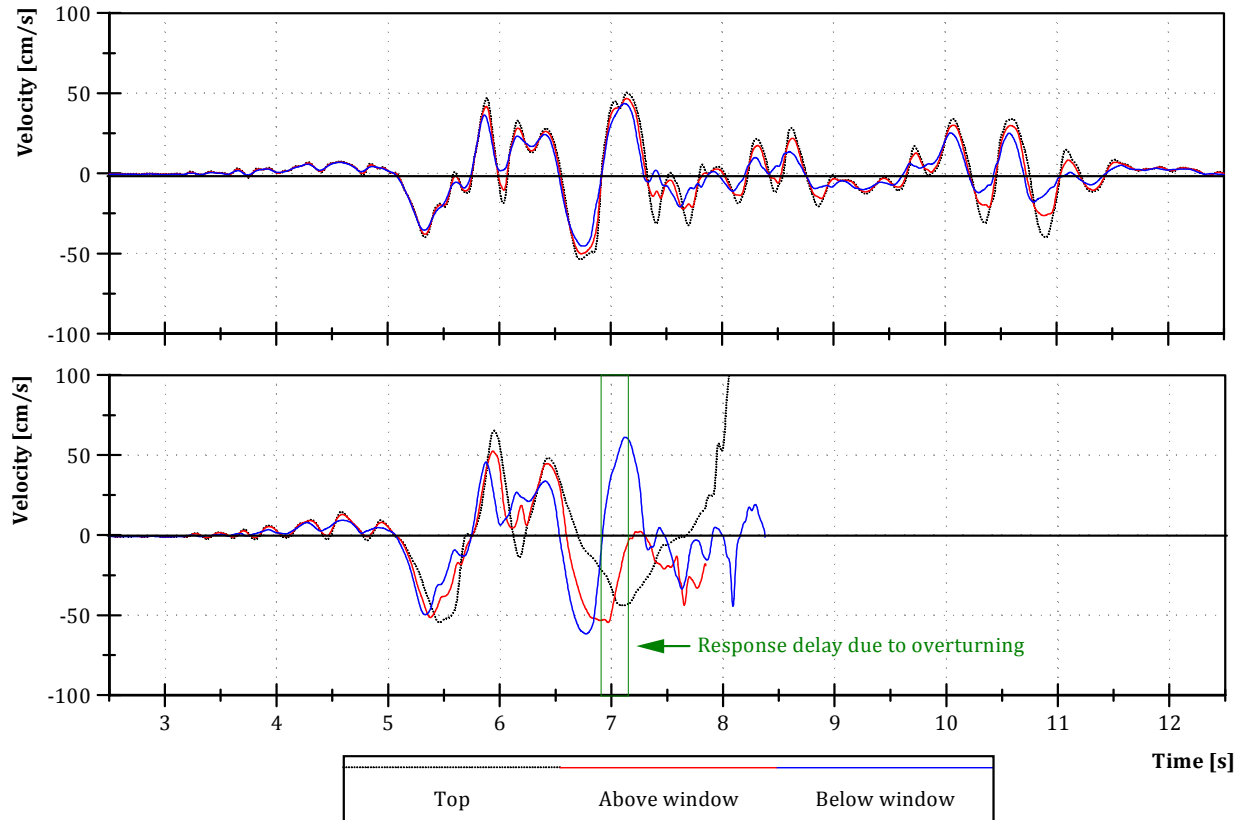


Figure 4.4. Velocity time histories: upper plot for stage L4 and lower plot for L5 test.

5. CONCLUSIONS

A full scale shaking table test was reported in this work, focusing on the out-of-plane behaviour of a *sacco* stone masonry façade with two returning walls. The tested specimen geometry and its properties were described as a partial reproduction of an existing stone masonry from Azores.

Moreover, the selection of the ground motion to be used on the shaking table was presented, which was an important component of the work to ensure the global overturning of the main façade without inducing severe damage in the tested construction.

Concerning the observed behaviour of the structure, the main objective of the experimental campaign was achieved with the out-of-plane collapse of the main façade for a PGA value of 0.48g. The window frame was found to be the most vulnerable element of the façade, particularly the window jamb stones due to their vertical orientation. It was also observed that the collapse was induced by instability of the outer leaf rather than the complete wall overturning. For this reason, it may be plausible suggesting that displacement-based assessment procedures concerning the out-of-plane behaviour of multiple-leaf masonry walls should consider the outer leaf thickness instead of the total wall thickness.

Finally, it is worth mentioning that the experimental data acquired in the shaking table tests allowed confirming both the rocking behaviour of the main façade and the modifications observed prior to collapse in stage L5.

ACKNOWLEDGEMENTS

This work refers research made with financial contribution of the Portuguese Foundation for Science and Technology (FCT) through the first author PhD grant (SFRH/BD/38138/2007).

Special acknowledgments are due to Laboratório Nacional de Engenharia Civil (LNEC), and to the technicians of the Laboratory for Earthquake and Structural Engineering (LESE) of the Faculty of Engineering of the University of Porto (FEUP).

REFERENCES

- Al Shawa, O., de Felice, G., Mauro, A. and Sorrentino, L. (2011). Out-of-plane seismic behaviour of rocking masonry walls. *Earthquake Engineering & Structural Dynamics* **41:5**, 949-968.
- Costa, A. (2002). Determination of mechanical properties of traditional masonry walls in dwellings of Faial island, Azores. *Earthquake Engineering and Structural Dynamics* **37:7**, 1361-1382.
- Costa, A.A. (2012). Seismic Assessment of the Out-of-Plane Performance of Traditional Stone Masonry Walls. Departamento de Engenharia Civil. Porto, Faculdade de Engenharia, Universidade do Porto. *Ph.D. Thesis*.
- D'Ayala, D. and Shi, Y. (2011). Modeling masonry historic buildings by multi-body dynamics. *International Journal of Architectural Heritage* **5:4-5**, 483-512.
- Decanini, L., Masiani, R., Sorrentino, L. and Tocci, C. (2006). Allegato 1.2-UR15-1: Risposta fuori del piano di pareti murarie, libere e vincolate in sommità, a settanta segnali naturali. Valutazione e riduzione della vulnerabilità di edifici in muratura. RELUIS. **(in italian)**.
- Lagomarsino, S. (1998). A new methodology for the post-earthquake investigation of ancient churches. *11th European Conference on Earthquake Engineering*, Paris, France, Balkema.
- Liberatore, D. and Santansiero, D. (2009). Oscillazioni di blocchi snelli sotto azione sismica: effetti del coefficiente di restituzione e della monolateralità. *ANIDIS 2009 - XIII Convegno di Ingegneria Sismica in Italia*, Bologna, Italy.
- Magenes, G., Penna, A. and Galasco, A. (2010). A full-scale shaking table test on a two-storey stone masonry building. *14th European Conference on Earthquake Engineering*, Ohrid, Macedonia.
- MSC (2012). ADAMS - Automatic Dynamic Analysis of Mechanical Systems, MSC Software Corporation.
- NTC (2008). Norme Tecniche per le Costruzioni, D. M. 14 gennaio 2008, Suppl. ord. n° 30 alla G.U. n. 29 del 4/02/2008, Consiglio Superiore dei Lavori Pubblici (in italian).
- Tomazevic, M., Lutman, M. and Petkovic, L. (1996). Seismic behavior of masonry walls: experimental simulation. *Journal of Structural Engineering* **122:9**, 1040-1047.
- Vasconcelos, G. and Lourenço, P.B. (2009). Experimental characterization of stone masonry in shear and compression. *Construction and Building Materials* **23:11**, 3337-3345.